SCIENCE CHINA
Earth Sciences

• RESEARCH PAPER •

December 2015 Vol.58 No.12: 2165–2174
doi: 10.1007/s11430-015-5222-3

Olivine versus peridotite during serpentinization: Gas formation

HUANG RuiFang[1,2*], SUN WeiDong[1†], DING Xing[3], LIU JinZhong[4] & PENG ShaoBang[5]

[1] *Key Laboratory of Mineralogy and Metallogeny, Guangzhou Institute of Geochemistry, Chinese Academy of Sciences, Guangzhou 510640, China;*
[2] *Key Laboratory of Marginal Sea Geology, South China Sea Institute of Oceanology, Chinese Academy of Sciences, Guangzhou 510301, China;*
[3] *State Key Laboratory of Isotope Geochemistry, Guangzhou Institute of Geochemistry, Chinese Academy of Sciences, Guangzhou 510640, China;*
[4] *State Key Laboratory of Organic Geochemistry, Guangzhou Institute of Geochemistry, Chinese Academy of Sciences, Guangzhou 510640, China;*
[5] *Zhongshan Research Institute of Environmental Protection, Zhongshan 528403, China*

Received August 27, 2015; accepted November 3, 2015; published online November 11, 2015

The dependence of starting materials and their initial grain sizes on the formation of gases (H_2, CH_4, C_2H_6 and C_3H_8) during serpentinization was investigated by conducting hydrothermal experiments at 311°C and 3 kbar on olivine and peridotite with initial grain sizes ranging from <30 to 177 μm. Hydrocarbons (CH_4, C_2H_6 and C_3H_8) were produced from reaction between dissolved CO_2 in the starting fluids and H_2 formed during serpentinization, which were analyzed by Gas Chromatography. It was found that olivine serpentinization produced much less H_2 and CH_4 compared with those after peridotite alteration, while their C_2H_6 and C_3H_8 were identical. For example, for olivine with initial grain sizes of <30 μm, the amounts of H_2 and CH_4 were 79.6 mmol/kg and 460 μmol/kg after 27 days, respectively. By contrast, the quantities of H_2 and CH_4 produced in experiment on peridotite with the same run duration were much larger, 119 mmol/kg and 1300 μmol/kg, respectively. This indicates that spinel and pyroxene in peridotite may increase the amounts of H_2 and hydrocarbons, possibly due to the catalytic effect of aluminum released by spinel and pyroxene during serpentinization. Moreover, the production of H_2 and hydrocarbons is negatively correlated with initial grain sizes of the starting material, with smaller amounts of H_2 and hydrocarbons for larger initial grain sizes, indicating that the kinetics of serpentinization influences the formation of H_2 and hydrocarbons, possibly because of the lack of catalytic minerals for the starting material with larger grain sizes. This study suggests that olivine cannot completely represent peridotite during serpentinization, and that H_2 and hydrocarbons in hydrothermal fields near the mid-ocean ridge may be produced in a very long period of serpentinization or the presence of catalytic minerals due to large grain sizes of ultramafic rocks.

serpentinization, hydrogen gas, hydrocarbon, olivine, peridotite

Citation: Huang R F, Sun W D, Ding X, Liu J Z, Peng S B. 2015. Olivine versus peridotite during serpentinization: Gas formation. Science China: Earth Sciences, 58: 2165−2174, doi: 10.1007/s11430-015-5222-3

Serpentinization, which is a low-temperature (≤500°C) hydrothermal alteration of ultramafic rocks (primary peridotite and komatiite), occurs widely in different tectonic settings on Earth, e.g., seafloor, slowly spreading mid-ocean ridges and subduction zones (Bloomer, 1983; Fryer et al., 1985; Charlou et al., 1996, 1998, 2000, 2002, 2010; Maekawa et al., 2001; Hyndman and Peacock, 2003; Mével, 2003), and also on Mars (e.g., Ehlmann et al., 2008, 2009, 2010). It is potentially significant for the origin and evolution of life during the early history of the Earth and possibly on other planets (e.g., Corliss et al., 1979, 1981; Schrenk et al., 2013; Wang et al., 2014), based on the observation that living organisms (e.g., bacteria, shrimps and crabs) survive in hydrothermal fields (e.g., Rainbow, Logachev and Lost City) those are provided with materials and energies from hydro-

*Corresponding author (email: rfhuang@gig.ac.cn)
†Corresponding author (email: weidongsun@gig.ac.cn)

gen gas, alkanes and organic acids produced during serpentinization (Kelley et al., 2001; Charlou et al., 1998, 2002, 2010; Holm and Charlou, 2001; Schrenk et al., 2004; Brazelton et al., 2006, 2010; Lang et al., 2010). Hydrogen gas forms after the reduction of hydrogen in water, and ferrous iron of olivine or pyroxene is oxidized to ferric iron (Reaction (1)). Reaction of hydrogen gas with oxidized carbon (e.g., CO, CO_2 or carbonate) forms abiotic hydrocarbons (such as CH_4, C_2H_6 and C_3H_8) (Fischer-Tropsch type (FTT) synthesis, Reaction (2)).

$$2Fe^{2+}+2H_2O=2Fe^{3+}+H_2+2OH^- \quad (1)$$

$$nCO_2+(3n+1)H_2=C_nH_{2n+2}+2nH_2O \quad (2)$$

Factors those affect the formation of hydrogen gas and alkanes during serpentinization have been explored by both experimental and thermodynamic studies (e.g., Berndt et al., 1996; Allen and Seyfried, 2003; McCollom and Seewald, 2001, 2003; McCollom and Bach, 2009; Oze et al., 2012; Huang et al., 2015a). Temperatures, water/rock ratios and the kinetics strongly influence H_2 production. Hydrogen gas is largest at ~300°C, which decreases dramatically at temperatures higher than 350°C due to the sluggish alteration rate of olivine (e.g., Berndt et al., 1996; Allen and Seyfried, 2003; McCollom and Bach, 2009). Moreover, the concentration of H_2 is negatively correlated with water/rock ratios, which becomes two orders of magnitude lower if water/rock ratios increase from 1 to 10 at 300°C (McCollom and Bach, 2009). Furthermore, the amount of H_2 is positively related with the reaction progress of serpentinization (e.g., Berndt et al., 1996; Marcaillou et al., 2011). On the other hand, the production of hydrocarbons is dramatically affected by catalytic minerals. Without the presence of catalytic minerals, only a very small percentage of CO_2 is converted into hydrocarbons (<1%, Berndt et al., 1996; McCollom and Seewald, 2001). However, catalytic minerals, such as Fe-Ni alloy, chromite and Co-bearing magnetite, enhance the production of hydrocarbons (Horita and Berndt, 1999; Foustoukos and Seyfried, 2004; Ji et al., 2008).

Olivine was taken as the starting material for most previous experiments to represent peridotite (e.g., Berndt et al., 1996; Oze et al., 2012). Indeed, olivine is one of the most abundant minerals in peridotite (typically >60%), and olivine serpentinization is the main serpentine-forming process at the early stage of serpentinization (e.g., Bach et al., 2006; Beard et al., 2009). However, peridotite serpentinization may produce larger quantities of H_2 and hydrocarbons, possibly caused by the presence of spinel and pyroxene, which release aluminum during serpentinization (e.g., Dungan, 1979; Hébert et al., 1990; Mellini et al., 2005; Huang et al., 2015b). Aluminum could dramatically enhance the reaction progress that is positively correlated with the quantity of H_2 (Marcaillou et al., 2011; Andreani et al., 2013). Moreover, more catalytic minerals may form with larger reaction progress, possibly inducing larger amounts of hydrocarbons. This is evidenced by experiments of Huang et al. (2015a) showing that more H_2 and CH_4 were produced at 500°C and 3 kbar during peridotite alteration than those after serpentinization of olivine or orthopyroxene, and H_2 formed mainly after orthopyroxene serpentinization. However, whether such trend could be observed at 300°C is unknown, during which H_2 is mostly produced after olivine serpentinization. Particularly, it is impossible to compare gas formation between olivine and peridotite serpentinization in previous experiments mainly due to different grain sizes, largely varied water/rock ratios, and distinct run time (e.g., Berndt et al., 1996; Allen and Seyfried, 2003; Marcaillou et al., 2011; Oze et al., 2012). On the other hand, the production of H_2 and hydrocarbons during serpentinization may depend on initial grain sizes of the starting material those strongly affect the kinetics of serpentinization (Martin and Fyfe, 1970; Wegner and Ernst, 1983; Malvoisin et al., 2012b), which has not been investigated yet. In this study, we conducted hydrothermal experiments at 311°C and 3 kbar on olivine and peridotite with initial grain sizes from <30 to 177 μm to compare the production of H_2 and hydrocarbons during serpentinization of olivine and peridotite, and to investigate the influence of initial grain sizes of the starting material on gas formation.

1 Materials and methods

1.1 Starting materials and capsule preparation

A non-altered spinel-bearing peridotite was chosen as the starting material. The peridotite was sampled at Panshishan (Jiangsu province, China) where it occurs as xenoliths in basalts (Chen et al., 1994; Sun et al. 1998; Xu et al., 2008; Yang, 2008). It is composed of olivine (60%–65%), orthopyroxene (20%–25%), clinopyroxene (15%) and spinel (1%–3%). Chemical compositions of the individual minerals were shown in Huang et al. (2015b), which is consistent with previous studies (Chen et al., 1994; Yang, 2008). Peridotite was crushed, ground in an agate motor and then sieved into grain sizes of <30 μm and 100–177 μm, respectively. Pure and clean olivine grains were picked from coarse peridotite powder under binocular microscope, which were then ground and sieved into grain sizes of <30 μm. The starting fluid was 0.5 mol/L NaCl that was prepared using fresh deionized water and reagent-grade sodium chloride.

Around 50 mg solid powders and ~50 mg starting fluids were loaded into gold capsules (30 mm long, 4.0 mm outer diameter and 0.2 mm wall thickness), which were sealed by arc welding. Leaks were checked before and after experiments by heating capsules in an oven at 100°C for several hours.

1.2 High pressure experiments

All the experiments were conducted in cold-seal hydrothermal

vessels with water as pressure medium at Guangzhou Institute of Geochemistry (Huang et al., 2015a, Table 1). The prepared capsule was loaded into the end of vessel followed with a filler rod (around 6 cm in length). Pressures were achieved by pumping water into the vessel and measured by a pressure gauge with precision of ±100 bar. Temperatures were monitored with an external K-type thermocouple that was inserted into a hole near the end of the vessel with the accuracy within 2°C. The vessels were immersed into ice water and the temperature of capsule decreased to <100°C within a few seconds.

1.3 Analytical methods

The gas components (H_2, CH_4, C_2H_6 and C_3H_8) were analyzed with an Agilent 7890A gas chromatography at the State Key Laboratory of Organic Geochemistry, Guangzhou Institute of Geochemistry. The gold capsule was put in a vacuum glass piercer connected to a Toepler pump and a volume-calibrated glass pipe through vacuum line. Before the capsule was pierced, the whole device was evacuated by a vacuum pump to reach the pressure of less than 1×10^{-2} Pa. Then the gold capsule was pierced by a steel needle in vacuum and all the gas components were concentrated by the Toepler pump into the volume-calibrated pipe. The pipe was attached to an Agilent 7890A gas chromatography, fitted with a HayeSep Q column (27 m×0.32 mm i.d.). Nitrogen was used as the carrier gas at a flow rate of 25 mL/min. The oven temperature was programmed as follows: 60°C for 3 min, raised from 60 to 180°C at 25°C/min, and then kept at 180°C for 3 min. A blank analysis was conducted before sample measurement for all samples. The gas components were quantified with an external standard, and the accuracy was less than 0.5%. The detailed analysis procedure has been reported in Xiong et al. (2001) and Pan et al. (2006).

The surface morphology of the experimental products was characterized with secondary electron using Zeiss Ultra 55 Field emission gun scanning electron microscope (FESEM). Samples were dispersed onto a double-sided carbon tape and coated with a thin film of platinum for FESEM observation.

Mineral compositions were determined using JOEL JXA 8100 electron microprobe with four wavelength-dispersive spectrometers at Second Institute of Oceanography, State Oceanic Administration. A 15 kV accelerating voltage, 20 nA beam current and 15 μm beam diameter were used. The calibration standards were jadite (Si, Na), olivine (Mg), almandine garnet (Fe, Al), diopside (Ca), sandine (K), chromium oxide (Cr), rutile (Ti), nickel silicide (Ni), cobalt metal (Co), rhodonite (Mn), and tugtupite (Cl). For Ni, Co, Cl and Mn, the counting time was 30 s/15 s for peak and background, respectively; for other elements, the counting time was 10 s/5 s for peak and background.

2 Results

2.1 Gas composition

Gas concentrations changed dramatically during experiment (Figure 1). In experiments on peridotite with initial grain sizes of <30 μm, H_2 gradually increased from 20 mmol/kg at 10 days to 167 mmol/kg at 14 days, while it slightly decreased to 119 mmol/kg at 27 days. Consistently, CH_4 reached 350 μmol/kg at 10 days, which rose to 2880 μmol/kg at 14 days but it decreased to 1300 μmol/kg at 27 days. The decrease of H_2 and CH_4 at 27 days is possibly due to the formation of organic acids, which were commonly produced during serpentinization and were not analyzed in this study (e.g., McCollom and Seewald, 2003).

In comparison, for experiments on olivine with initial grain sizes of <30 μm, the concentration of H_2 reached 94.5 mmol/kg at 10 days, while it largely decreased to 2.8 mmol/kg at 14 days and then it rose to 79.6 mmol/kg at

Table 1 Composition of gases produced in serpentinization experiments at 3 kbar and 311°C [a)]

Sample No.	Starting material	Initial grain sizes (μm)	W/R ratio	Duration (days)	H_2 (mmol/kg)	CH_4 (μmol/kg)	C_2H_6 (μmol/kg)	C_3H_8 (μmol/kg)
HR61	Prt	100–177	0.82	120	127	60	2.72	5.4
HR77	Prt	100–177	1.2	28	10	28	26.5	39.5
HR105	Prt	<30	1.0	10	21	350	23.6	9.2
HR91	Prt	<30	0.89	14	167	2880	161.4	321.8
HR86	Prt	<30	0.86	27	119	1300	59.3	316.8
HR76	Ol	<30	1.04	27	80	460	136.4	234.9
HR87	Ol	<30	0.71	14	3	1680	121.6	0.69
HR106	Ol	<30	0.90	10	94	260	37.1	116.0
Fe37	Ol	100–177	1.1	26	10	0.0	0.0	0.0
HR25	Prt	100–177	1.4	19	–	–	–	–

a) Prt=peridotite, Ol=olivine; W/R ratio: Ratio of the mass of initial fluids and that of solid materials loaded in capsules; Fe37 data are from Huang et al. (2015a).

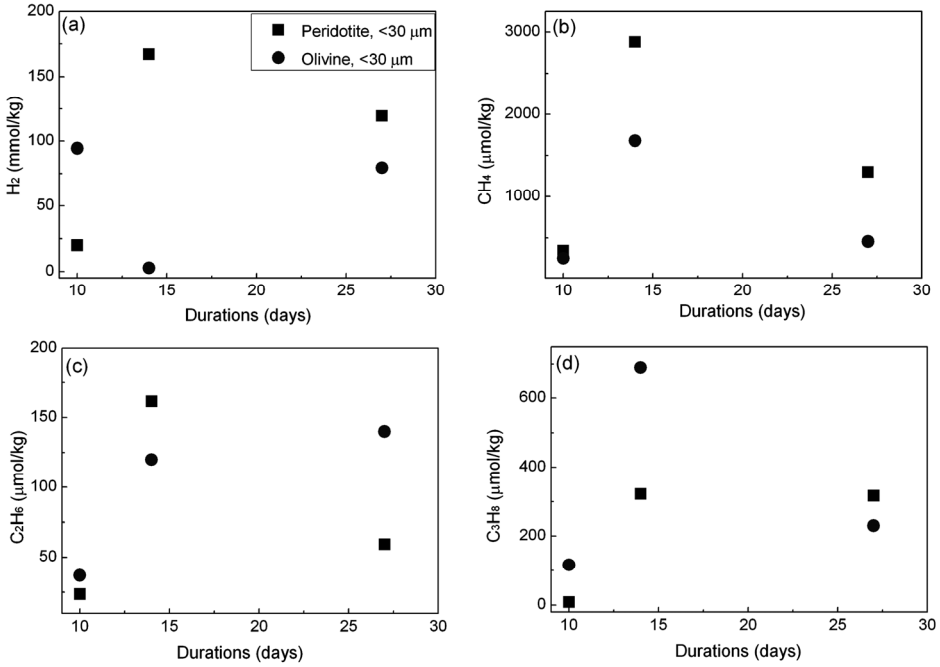

Figure 1 Comparison of gas formation during olivine and peridotite serpentinization. Larger amounts of H_2 and CH_4 were produced during peridotite serpentinization, while their C_2H_6 and C_3H_8 were identical.

27 days. By contrast, the quantity of methane as a function of time shows an opposite trend, which was very low at 10 days, and increased greatly at 14 days, and then decreased at 27 days, indicating that the decrease of H_2 at 14 days is due to the formation of methane and other hydrocarbons. Compared with olivine, peridotite alteration produced a larger quantity of CH_4 (Figure 1), while their C_2H_6 and C_3H_8 were identical. At 10 days, peridotite serpentinization generated less H_2 than olivine alteration (Figure 1). However, with progressive serpentinization (at 14 and 27 days), the amount of H_2 was much larger during peridotite serpentinization compared with that after olivine alteration.

The production of H_2 and hydrocarbons strongly depends on initial grain sizes of the starting material, with larger amounts of H_2 and hydrocarbons for smaller grain sizes of peridotite (Figure 2). For example, in experiments taking peridotite with grain sizes of <30 μm, the quantities of H_2 and CH_4 at 27 days were 119 mmol/kg and 1300 μmol/kg, respectively. By contrast, for those with larger grain sizes (100–177 μm), the concentrations of H_2 and hydrocarbons at 28 days were one to three orders of magnitude smaller. With progressive serpentinization (120 days), the quantity of H_2 was identical to that using peridotite with smaller grain sizes, while the amounts of hydrocarbons were almost the same as those at 28 days, indicating that the production of H_2 and hydrocarbons during serpentinization has two stages. At the early stage, the rate of H_2 production is fast, while that of CH_4 formation is very slow. During the second stage, the amount of CH_4 gradually increases, whereas that of H_2 almost keeps constant or slightly decreases, which is consistent with Oze et al. (2012).

2.2 Solid run products

The run products were composed of fibrous chrysotile, (±) lizardite, and (±) magnetite grains (Figure 3). Chrysotile was characterized by FTIR bands at 615, 954 and 3689 cm^{-1} (Figure 4, Anbalagan et al., 2010). The diameter of chrysotile was positively related with initial grain sizes of the starting material (Figure 3(a), (b)). Magnetite sizes ranged from less than 1 μm to around 10 μm. It appears that more magnetite grains crystallized during olivine serpentinization (Figure 3(c), (d)). As a consequence, serpentine formed in experiments taking olivine contained 5.9±2.0 wt.% FeO (Table 2), much less than those of primary olivine (9.8 wt.%). By contrast, serpentine crystallized in those using peridotite had much larger iron contents, 8.2±1.6 wt.% FeO (Table 2).

3 Discussion

The carbon source of this study is the dissolved CO_2 from the atmosphere, ~0.60 mmol/kg after experiments, which is identical with previous studies (McCollom and Seewald, 2001; Oze et al., 2012). Although such CO_2 is much less than that produced after the breakdown of bicarbonate (e.g., Berndt et al., 1996), it is large enough for FTT synthesis due to the small conversion percentage of CO_2 into hydrocarbons. Moreover, the production of hydrocarbons was not promoted by slightly higher CO_2 in the reaction system (e.g., Berndt et al., 1996; McCollom and Seewald, 2001; Huang et al., 2015a). Particularly, with the presence of even higher CO_2, the quantities of H_2 and CH_4 became smaller due to

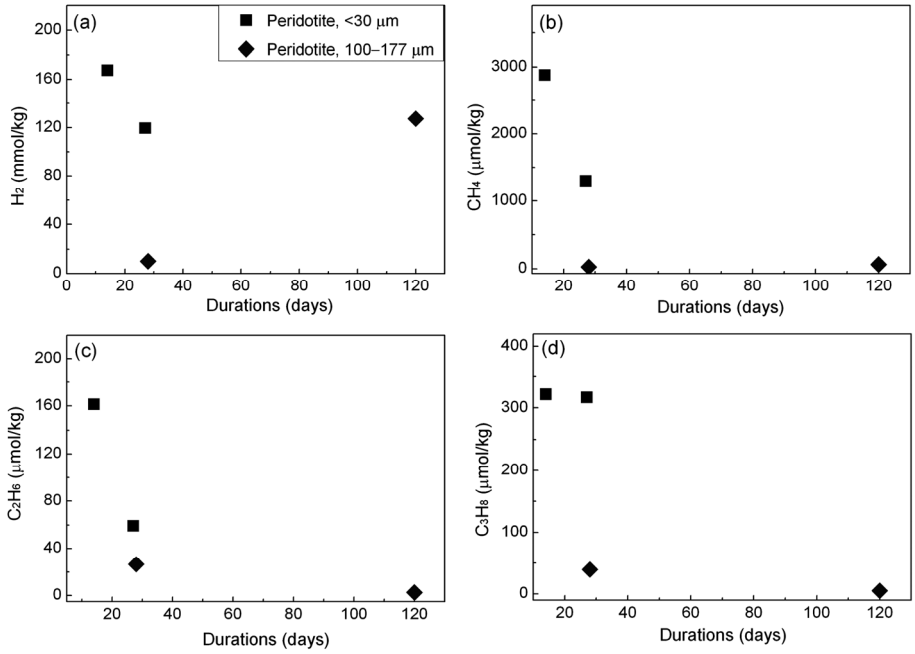

Figure 2 Grain-size dependence of the formation of H_2 and hydrocarbons during peridotite serpentinization. The quantities of H_2 and hydrocarbons were negatively correlated with grain sizes of the starting peridotite, with smaller amounts of gases for larger grain sizes of peridotite.

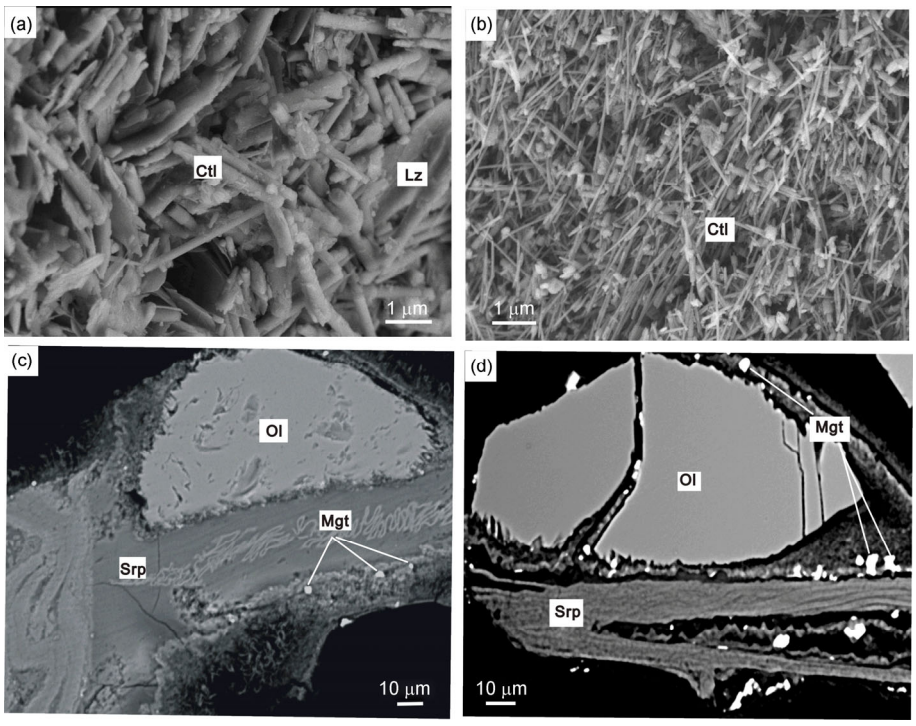

Figure 3 Typical run products of (a) HR61, peridotite with grain sizes of 100–177 μm; (b) HR76, olivine with grain sizes of <30 μm; (c) HR25, peridotite with grain sizes of 100–177 μm and (d) Fe-37, olivine with grain sizes of 100–177 μm. The major run products are fibrous chrysotile, (±) lizardite and magnetite. The diameter of chrysotile is positively related with the initial grain sizes of the starting material. It seems that more magnetite grains form during olivine serpentinization (d) than those produced during peridotite alteration (c). Ctl=chrysotile; Lz=lizardite; Ol=olivine; Srp=serpentine; Mgt=magnetite.

the incorporation of Fe^{2+} into carbonates (Jones et al., 2010). On the other hand, olivine as the carbon source was excluded due to its low carbon solubility (<1 ppm) (Keppler et al., 2003).

To investigate whether hydrogen gas and hydrocarbons were produced during serpentinization and FTT synthesis or after decomposition of long-chain hydrocarbons in primary peridotite (e.g., Tingle et al., 1990; Sugisaki and Mimura,

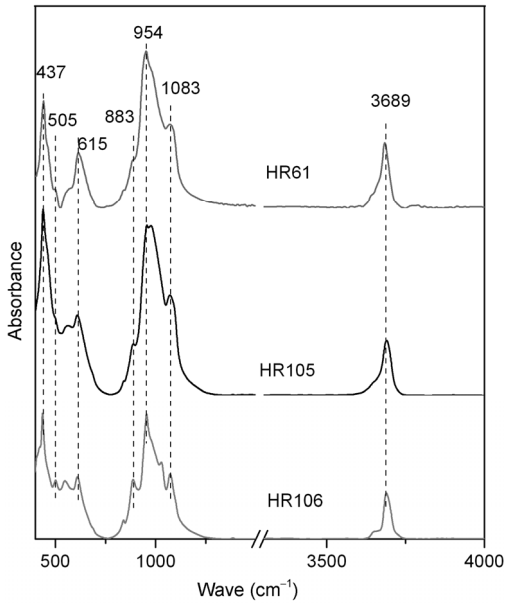

Figure 4 FTIR spectra of run products. Chrysotile, the major product in most experiments, is characterized with 615, 954 and 3689 cm^{-1} (e.g., Anbalagan et al., 2010), while residual olivine is characterized with peaks at 505 and 883 cm^{-1} (e.g., Jeanloz, 1980).

Table 2 Typical chemical composition of serpentine analyzed by electron microprobe

Sample No.	HR25	HR61	Fe37
SiO_2	39.35	38.43	38.09
TiO_2	0.10	0.05	0.00
Cr_2O_3	0.04	0.47	0.06
Al_2O_3	2.42	1.79	0.49
MgO	34.95	35.76	36.91
FeO	8.81	6.38	4.88
MnO	0.10	0.08	0.05
NiO	0.24	0.08	0.26
CaO	0.10	0.24	0.06
K_2O	0.01	0.00	0.02
Na_2O	0.19	0.19	0.00
Cl	0.10	0.19	0.17
Total	86.39	83.61	80.95

1994), we conducted blank experiments at 300–500°C and 3 kbar taking olivine or peridotite with initial grain sizes of <30 μm without adding any fluids. The quantities of H_2 and hydrocarbons at 27 days were below the detection limit of gas chromatography, indicating that olivine and peridotite taken in this study contain no H_2 and hydrocarbons, or that they have such gases those were stable during the run. Therefore, the detected H_2 and hydrocarbons in hydrothermal experiments were formed due to the reaction between olivine or peridotite and the starting fluid rather than from the breakdown of long-chain hydrocarbons in primary ultramafic rocks.

Peridotite serpentinization produces more H_2 and CH_4 than olivine alteration (Figure 1), indicating that olivine cannot completely represent peridotite during serpentinization, possibly caused by pyroxene and spinel. However, orthopyroxene serpentinization at ~300°C and 3 kbar produced even less H_2 compared with that after olivine alteration, and no H_2 and hydrocarbons were detected after clinopyroxene hydration (Huang et al., 2015a). Why pyroxene and spinel promote the production of hydrogen gas and alkanes during olivine serpentinization? One possible way is that pyroxene and spinel could modify chemical compositions of serpentinization fluids, which consequently enhances the formation of hydrogen gas and alkanes. Compared with olivine, peridotite has higher silica contents, and fluids during peridotite serpentinization are more enriched in silica. However, the possibility that larger silica contents induce more H_2 and CH_4 is excluded based on the detection of even less H_2 in most natural hydrothermal fluids with larger silica contents (Charlou et al., 2002, 2010; Seyfried et al., 2011). Moreover, olivine is deficient in aluminum, while pyroxene and spinel of peridotite are rich in aluminum. Particularly, pyroxene and spinel released aluminum during serpentinization (Dungan, 1979; Hébert et al., 1990; Huang et al., 2015b). It has been reported that pyroxene lost some of aluminum to its neighboring olivine during serpentinization, indicated by Al-rich serpentine after olivine alteration (Dungan, 1979; Hébert et al., 1990; Huang et al., 2015b). Furthermore, spinel occurring in serpentinites is commonly altered to Al- poor ferrichromite and (±) magnetite rinds (e.g., Mellini et al., 2005). All these indicate that aluminum is mobile during peridotite serpentinization, and that it could be released by pyroxene and spinel. Aluminum speeds up the alteration rate of olivine serpentinization (Andreani et al., 2013), resulting in a larger reaction progress. The quantity of H_2 is positively correlated with the reaction progress (Marcaillou et al., 2011), and therefore aluminum may dramatically increase the production of H_2. Additionally, compared with olivine, pyroxene and spinel are rich in chromium. It has been shown that chromium could be leached into fluids even at ambient temperature those are in equilibrium with chromite or Cr_2O_3 (Ulmer, 1974), and a larger quantity of chromium was released at higher temperatures and pressures (Klein-BenDavid et al., 2011). Pyroxene, especially clinopyroxene, lost most of its chromium into fluids, indicated by Cr-depleted serpentine derived from clinopyroxene (e.g., Hébert et al., 1990). All these suggest that chromium could be released by spinel and pyroxene during serpentinization. Chromium catalyzes the production of CH_4, C_2H_6 and C_3H_8 during FTT synthesis (Foustoukos and Seyfried, 2004). However, the effect of chromium and spinel on the formation of hydrocarbons may need further investigation, due to the ambiguity of the catalytic effect of natural-occurring chromite (Lazar et al., 2012; Oze et al., 2012).

The production of H_2 and hydrocarbons strongly depends on initial grain sizes of the starting material, with larger amounts of H_2 and hydrocarbons for smaller grain sizes

(Figure 2). Initial grain sizes of the starting material are negatively correlated with the kinetics of serpentinization (Wegner and Ernst, 1983; Malvoisin et al., 2012b), and peridotite with smaller grain sizes has a larger reaction progress. The production of H_2 is positively correlated with the serpentinization progress (Marcaillou et al., 2011), and therefore serpentinization of peridotite with smaller initial grain sizes could induce a larger amount of H_2. Meanwhile, more catalytic minerals may be produced with larger reaction progress, possibly resulting in more CH_4. The catalytic minerals may be aluminum, Fe-Ni alloy and magnetite. The potential catalytic effect of aluminum is indicated by more CH_4 formed after peridotite serpentinization than that during olivine alteration. Iron-Ni alloy is a common accessory mineral in serpentinites, which efficiently catalyzes the production of CH_4, while it has no influence on other hydrocarbons (Horita and Berndt, 1999). Additionally, magnetite has been proposed to catalyze the formation of hydrocarbons (e.g., Berndt et al., 1996), while experiments with ^{13}C-rich fluids showed that magnetite cannot increase the production of $^{13}CH_4$ and other ^{13}C-rich hydrocarbons (McCollom and Seewald, 2001, 2003).

Moreover, the production of H_2 and hydrocarbons during olivine serpentinization also strongly depends on initial grain sizes of olivine (e.g., Berndt et al., 1996; Oze et al., 2012; Huang et al., 2015a). For example, the experiment of Berndt et al. (1996) was conducted at 300°C and 0.5 kbar taking olivine with initial grain sizes of ⩽75 μm, and the quantity of CH_4 (37 μmol/kg) was much smaller than that of this study using olivine with smaller grain sizes (<30 μm, 460 μmol/kg) (Berndt et al., 1996). Consistently, the quantities of H_2 (~4 mmol/kg) and CH_4 (60 μmol/kg) formed in Oze et al. (2012) taking olivine with initial grain sizes of 100 μm were two orders of magnitude less than those of this study. Although water/rock ratios of previous experiments are twice of those in this study (Berndt et al., 1996; Oze et al., 2012), such difference probably cannot induce the large contrast of H_2 and CH_4. As indicated by McCollom and Bach (2009), the concentration of H_2 becomes two orders of magnitude lower if water/rock ratios increase from 1 to 10 at 300°C. Therefore, initial grain sizes of the starting material may be more controlling compared with water/rock ratios. Particularly, the water/rock ratio of experiment in Huang et al. (2015a) is 1.1 (Fe37, Table 1), identical with that of this study. However, the quantity of H_2 after alteration of olivine with grain sizes of 100–177 μm was 10 mmol/kg after 26 days (Fe37, Huang et al., 2015a), much smaller than that formed during serpentinization of olivine with smaller grain sizes, indicating that the formation of gases during serpentinization is strongly affected by initial grain sizes of the starting material.

However, grain-size dependence was not observed in Marcaillou et al. (2011), who conducted experiments at 300°C and 0.3 kbar taking ground peridotite with initial grain sizes of <1 μm. H_2 was only 39 mmol/kg after 34 days, much less than that produced in this study (119 mmol/kg, HR86). It is possibly because their experiments were performed in a steel autoclave (Marcaillou et al., 2011), which may react with serpentinization fluids during the run (e.g., Okamoto et al., 2011), possibly influencing H_2 production. Moreover, the major run product of Marcaillou et al. (2011) was lizardite, while that of this study was chrysotile. It has been shown that chrysotile crystallization requires a higher degree of solution supersaturation than lizardite (e.g., Normand et al., 2002), and therefore the serpentinization processes may be different.

Not only gas formation, magnetite production during olivine serpentinization may be distinct from that after peridotite alteration. Serpentine produced after peridotite serpentinization of this study is more enriched in iron than that formed during olivine alteration (Table 2), implying that less magnetite was produced during peridotite serpentinization. There are two possible explanations for the less amounts of magnetite. First, peridotite has higher SiO_2 contents under which condition magnetite is unstable (Frost and Beard, 2007; Reaction (3)).

$$\underset{\text{serpentine}}{2Fe_3Si_2O_5(OH)_4}+O_2=\underset{\text{magnetite}}{2Fe_3O_4}+\underset{\text{silica}}{4SiO_2}+4H_2O \quad (3)$$

Another possibility is that olivine lost some of its iron to clinopyroxene during peridotite serpentinization, indicated by the production of Fe-rich serpentine after clinopyroxene alteration (Huang et al., 2015b), possibly resulting in less magnetite. The difference of magnetite formation between olivine and peridotite serpentinization is also indicated by previous studies (e.g., Toft et al., 1990; Oufi et al., 2002; Okamoto et al., 2011, Malvoisin et al., 2012b). Magnetite crystallized during olivine serpentinization within 24 hours (e.g., Okamoto et al., 2011, Malvoisin et al., 2012b), and the amount of magnetite is linearly correlated with the reaction progress (Malvoisin et al., 2012a, 2012b). By contrast, the quantity of magnetite was very low during the early stage of peridotite serpentinization, which increased abruptly when the reaction progress exceeded 75% (Toft et al., 1990; Oufi et al., 2002). More experiments are preferred in future studies.

Moreover, serpentine formed after peridotite serpentinization probably contains more Fe^{3+} than that produced during olivine hydration, indicated by a larger quantity of H_2 formed during peridotite serpentinization. The production of H_2 results in Fe^{3+} formation (Reaction (1)), which is either incorporated into serpentine or magnetite. The less magnetite during peridotite serpentinization indicates the formation of Fe^{3+}-rich serpentine.

Hydrogen gas and hydrocarbons were commonly detected in natural hydrothermal fluids, which formed during serpentinization of ultramafic basement rocks (e.g., Charlou et al., 1996, 1998, 2000, 2002; Douville et al., 2002). Typically, the quantity of H_2 was smaller than that produced in experiments on olivine serpentinization, while the amount of CH_4 was larger (e.g., Berndt et al., 1996; Douville et al.,

2002). For example, the concentrations of H_2 and CH_4 in fluids from Rainbow hydrothermal fields were 16 mmol/kg and 2.5 mmol/kg, respectively (Douville et al., 2002). In principle, a smaller amount of CH_4 may be produced in hydrothermal fields due to larger grain sizes of ultramafic rocks. The larger quantity of CH_4 indicates the presence of catalytic minerals or much longer serpentinization time. Nevertheless, the influence of initial grain sizes of the starting material should not be ignored. For example, Oze et al. (2012) investigated the catalytic effect of naturally occurring chromite on FTT synthesis by comparing chromite-free with-bearing experiments. It was found that chromite cannot enhance the production of alkanes (Oze et al., 2012), in contrast with Foustoukos and Seyfried (2004). However, the low quantities of hydrogen gas and alkanes may be induced by large grain sizes of olivine (100 μm) and short run durations (around 33 days) (Oze et al., 2012), and whether chromite could catalyze the production of alkanes during FTT synthesis still needs further investigation. Considering a long period of serpentinization or smaller initial grain sizes of olivine, chromite may promote the formation of alkanes. On the other hand, the smaller amount of H_2 is possibly caused by gas escaping, indicated by gas bubbling in the hydrothermal systems of Prony Bay (Monnin et al., 2014).

4 Conclusion

Hydrogen gas and hydrocarbons form during serpentinization and FTT synthesis, which may be significant for the origin and evolution of life during the early history and the Earth and possibly on other planets (e.g., Kelley et al., 2001; Holm and Charlou, 2001; Schrenk et al., 2004, 2013; Brazelton et al., 2006, 2010; Lang et al., 2010; Wang et al., 2014). Most previous experiments were conducted taking olivine to represent peridotite. However, this study shows that much larger amounts of H_2 and CH_4 were produced during peridotite serpentinization compared with those after olivine alteration, probably caused by spinel and pyroxene those release aluminum and chromium during serpentinization and may consequently catalyze the formation of H_2 and CH_4. It indicates that olivine cannot completely represent peridotite during serpentinization, and comparisons of other aspects between olivine and peridotite hydration will be investigated in our later studies. Moreover, initial grain sizes of the starting material could largely affect the production of H_2 and hydrocarbons during serpentinization, with larger grain sizes for less H_2 and hydrocarbons. It may take a very long period of time for natural hydrothermal fields to reach the present quantities of H_2 and hydrocarbons due to large grain sizes of ultramafic rocks.

We thank Li Yong of Guangzhou Institute of Geochemistry for the assistance during GC analyses. We appreciated Prof. I-Ming Chou and two other anonymous reviewers' comments and suggestions, which are constructive for the manuscript. This work was financially supported by the National Natural Science Foundation of China (Grant Nos. 41090373, 41121002, 41103012 and 41173069), the Strategic Priority Research Program of the Chinese Academy of Sciences (Grant No. XDB06030100), and also by Postdoctoral Science Foundation of China (Grant No. 2015M570735).

Allen D E, Seyfried W E Jr. 2003. Compositional controls on vent fluids from ultramafic-hosted hydrothermal systems at mid-ocean ridges: An experimental study at 400°C, 500 bars. Geochim Cosmochim Acta, 67: 1531–1542

Anbalagan G, Sivakumar G, Prabakaran A R, Gunasekaran S. 2010. Spectroscopic characterization of natural chrysotile. Vib Spectrosc, 52: 122–127

Andreani M, Daniel I, Pollet-Villard M. 2013. Aluminum speeds up the hydrothermal alteration of olivine. Am Mineral, 98: 1738–1744

Bach W, Paulick H, Garrido C J, Ildefonse B, Meurer W P, Humphris S E. 2006. Unraveling the sequence of serpentinization reactions: Petrology, mineral chemistry, and petrophysics of serpentinites from MAR 15°N (ODP Leg 209, Site 1274). Geophys Res Lett, 33: L13306, doi: 10.1029/2006GL025681

Beard J S, Frost B R, Fryer P, McCaig A, Searle R, Ildefonse B, Zinin P, Sharma S K. 2009. Onset and progression of serpentinization and magnetite formation in olivine-rich troctolite from IODP Hole U1309D. J Petrol, 50: 387–403

Berndt M E, Allen D E, Seyfried W E Jr. 1996. Reduction of CO_2 during serpentinization of olivine at 300°C and 500 bar. Geology, 24: 351–354

Bloomer S H. 1983. Distribution and origin of igneous rocks from the landward slopes of the Mariana trench: Implications for its structure and evolution. J Geophys Res, 88: 7411–7428

Brazelton W J, Schrenk M O, Kelley D S, Baross J A. 2006. Methane- and sulfur-metabolizing microbial communities dominate the Lost City Hydrothermal Field ecosystem. Appl Environ Microbiol, 72: 6257–6270

Brazelton W J, Nelson B, Schrenk M O. 2010. Metagenomic evidence for H_2 oxidation and H_2 production by serpentinite-hosted subsurface microbial communities. Front Microbiol, 2: 1–16

Charlou J L, Fouquet Y, Donval J P, Auzende J M, Jean-Baptiste P, Stievenard M, Michel S. 1996. Mineral and gas chemistry of hydrothermal fluids on an ultrafast spreading ridge: East Pacific rise, 17° to 19°S (Naudur cruise, 1993) phase separation processes controlled by volcanic and tectonic activity. J Geophys Res, 101: 15899–15919

Charlou J L, Fouquet Y, Bougault H, Donval J P, Etoubleau J, Jean- Baptiste P, Dapoigny A, Appriou P, Rona P A. 1998. Intense CH_4 plumes generated by serpentinization of ultramafic rocks at the intersection of the 15°20′N fracture zone and the Mid-Atlantic Ridge. Geochim Cosmochim Acta, 62: 2323–2333

Charlou J L, Donval J P, Douville E, Jean-Baptiste P, Radford-Knoery J, Fouquet Y, Dapoigny A, Stievenard M. 2000. Compared geochemical signatures and the evolution of Menez Gwen (37°50′N) and Lucky Strike (37°17′N) hydrothermal fluids, south of the Azores triple junction on the Mid-Atlantic Ridge. Chem Geol, 171: 49–75

Charlou J L, Donval J P, Fouquet Y, Jean-Baptiste P, Holm N. 2002. Geochemistry of high H_2 and CH_4 vent fluids issuing from ultramafic rocks at the Rainbow hydrothermal field (36°14′N, MAR). Chem Geol, 191: 345–359

Charlou J L, Donval J P, Konn C, Ondréas H, Fouquet Y. 2010. High production and fluxes of H_2 and CH_4 and evidence of abiotic hydrocarbon synthesis by serpentinization in ultramafic-hosted hydrothermal systems on the Mid-Atlantic Ridge. Washington D C: American Geophysical Union

Chen D G, Li B X, Zhi X C. 1994. Genetic geochemistry of mantle-derived peridotite xenolith from Panshishan, Jiangsu. Geochimica, 23: 13–24

Corliss J B, Dymond J, Gordon L I, Edmond J M, von Herzen R P, Ballard R D, Green K, Williams D, Bainbridge A, Crane K, van Andel T H. 1979. Submarine thermal springs on the Galápogos rift. Science, 203: 1073–1083

Corliss J B, Baross J A, Hoffman S E. 1981. An hypothesis concerning the

relationship between submarine hot springs and the origin of life on Earth. Oceanol Acta, 4: 59–69

Douville E, Charlou J L, Oelkers E H, Bienvenu P, Jove Colon C F, Donval J P, Fouquet Y, Prieur D, Appriou P. 2002. The rainbow vent fluids (36°14′N, MAR): The influence of ultramafic rocks and phase separation on trace metal content in Mid-Atlantic Ridge hydrothermal fluids. Chem Geol, 184: 37–48

Dungan M A. 1979. A microprobe study of antigorite and some serpentine pseudomorphs. Can Mineral, 17: 771–784

Ehlmann B L, Mustard J F, Murchie S L, Poulet F, Bishop J L, Brown A J, Calvin W M, Clark R N, Des Marais D J, Milliken R E, Roach L H, Roush T L, Swayze G A, Wray J J. 2008. Orbital identification of carbonate-bearing rocks on Mars. Science, 322: 1828–1832

Ehlmann B L, Mustard J F, Swayze G A, Clark R N, Bishop J L, Poulet F, Des Marais D J, Roach L H, Milliken R E, Wray J J, Barnouin-Jha O, Murchie S L. 2009. Identification of hydrated silicate minerals on Mars using MRO-CRISM: Geologic context near Nili Fossae and implications for aqueous alteration. J Geophys Res, 114: E00D08, doi: 10.1029/2009JE003339

Ehlmann B L, Mustard J F, Murchie S L. 2010. Geologic setting of serpentine deposits on Mars. Geophys Res Lett, 37: L06201, doi: 10.1029/2010GL042596

Foustoukos D I, Seyfried W E Jr. 2004. Hydrocarbons in hydrothermal vent fluids: The role of chromium-bearing catalysts. Science, 304: 1002–1005

Frost B R, Beard J S. 2007. On silica activity and serpentinization. J Petrol, 48: 1351–1368

Fryer P, Ambos E L, Hussong D M. 1985. Origin and emplacement of Mariana forearc seamounts. Geology, 13: 774–777

Hébert R, Adamson A C, Komor S C. 1990. Metamorphic petrology of ODP Leg 109, Hole 670A serpentinized peridotites: Serpentinization processes at a slow spreading ridge environment. In: Proceedings of the Ocean Drilling Program. Scientific Results, 106/109: 103–115

Holm N G, Charlou J L. 2001. Initial indications of abiotic formation of hydrocarbons in the Rainbow ultramafic hydrothermal system, Mid-Atlantic Ridge. Earth Planet Sci Lett, 191: 1–8

Horita J, Berndt M E. 1999. Abiogenic methane formation and isotopic fractionation under hydrothermal conditions. Science, 285: 1055–1057

Huang R F, Sun W D, Ding X, Liu J Q, Zhan W H. 2015a. Formation of hydrogen gas and alkane during peridotite serpentinization. Acta Petrol Sin, 31: 1901–1907

Huang R F, Sun W D, Ding X, Wang Y R, Zhan W H. 2015b. Experimental investigation of iron mobility during serpentinization. Acta Petrol Sin, 31: 883–890

Hyndman R D, Peacock S M. 2003. Serpentinization of the forearc mantle. Earth Planet Sci Lett, 212: 417–432

Jeanloz R. 1980. Infrared spectra of olivine polymorphs: α, β phase and spinel. Phys Chem Minerals, 5: 327–341

Ji F W, Zhou H Y, Yang Q H. 2008. The abiotic formation of hydrocarbons from dissolved CO_2 under hydrothermal conditions with cobalt-bearing magnetite. Orig Life Evol Biosph, 38: 117–125

Jones L C, Rosenbauer R, Goldsmith J I, Oze C. 2010. Carbonate control of H_2 and CH_4 production in serpentinization systems at elevated P-Ts. Geophys Res Lett, 37: L14306, doi: 10.1029/2010GL043769

Kelley D S, Karson J A, Blackman D K, Früh-Green G L, Butterfield D A, Lilley M D, Olson E J, Schrenk M O, Roe K K, Lebon G T, Rivizzigno P, the AT3-60 shipboard party. 2001. An off-axis hydrothermal vent field near the Mid-Atlantic Ridge at 30°N. Nature, 412: 145–149

Keppler H, Wiedenbeck M, Shcheka S S. 2003. Carbon solubility in olivine and the mode of carbon storage in the Earth's mantle. Nature, 424: 414–416

Klein-BenDavid O, Pettke T, Kessel R. 2011. Chromium mobility in hydrous fluids at upper mantle conditions. Lithos, 125: 122–130

Kumagai H, Nakamura K, Toki T, Morishita T, Okino K, Ishibashi J I, Tsunogai U, Kawagucci S, Gamo T, Shibuya T, Sawaguchi T, Neo N, Joshima M, Sato T, Takai K. 2008. Geological background of the Kairei and Edmond hydrothermal fields along the Central Indian Ridge: Implications of their vent fluids' distinct chemistry. Geofluids, 8: 239–251

Lang S Q, Butterfield D A, Schulte M, Kelley D S, Lilley M D. 2010. Elevated concentrations of formate, acetate and dissolved organic carbon found at the Lost City hydrothermal field. Geochim Cosmochim Acta, 74: 941–952

Lazar C, McCollom T M, Manning C E. 2012. Abiogenic methanogenesis during experimental komatiite serpentinization: Implications for the evolution of the early Precambrian atmosphere. Chem Geol, 326–327: 102–112

Maekawa H, Yamamoto K, Teruaki I, Ueno T, Osada Y. 2001. Serpentinite seamounts and hydrated mantle wedge in the Izu-Bonin and Mariana forearc regions. Bull Earthq Res Inst, Univ Tokyo, 76: 355–366

Malvoisin B, Carlut J, Brunet F. 2012a. Serpentinization of oceanic peridotites: 1. A high-sensitivity method to monitor magnetite production in hydrothermal experiments. J Geophys Res, 117: B01104, doi: 10.1029/2011JB008612

Malvoisin B, Brunet F, Carlut J, Rouméjon S, Cannat M. 2012b. Serpentinization of oceanic peridotites: 2. Kinetics and progresses of San Carlos olivine hydrothermal alteration. J Geophys Res, 117: B04102, doi: 10.1029/2011JB008842

Marcaillou C, Muñoz M, Vidal O, Parra T, Harfouche M. 2011. Mineralogical evidence for H_2 degassing during serpentinization at 300°C/300 bar. Earth Planet Sci Lett, 303: 281–290

Martin B, Fyfe W S. 1970. Some experimental and theoretical observations on the kinetics of hydration reactions with particular reference to serpentinization. Chem Geol, 6: 185–202

McCollom T M, Seewald J S. 2001. A reassessment of the potential for reduction of dissolved CO_2 to hydrocarbons during serpentinization of olivine. Geochim Cosmochim Acta, 65: 3769–3778

McCollom T M, Seewald J S. 2003. Experimental constraints on the hydrothermal reactivity of organic acids and acid anions: I. Formic acid and formate. Geochim Cosmochim Acta, 67: 3625–3644

McCollom T M, Bach W. 2009. Thermodynamic constraints on hydrogen generation during serpentinization of ultramafic rocks. Geochim Cosmochim Acta, 73: 856–875

Mellini M, Rumori C, Viti C. 2005. Hydrothermally reset magmatic spinels in retrograde serpentinites: Formation of "ferritchromit" rims and chlorite aureoles. Contrib Mineral Petr, 149: 266–275

Mével C. 2003. Serpentinization of abyssal peridotites at mid-ocean ridges. C R Geosci, 335: 825–852

Monnin C, Chavagnac V, Boulart C, Ménez B, Gérard M, Gérard E, Pisapia C, Quéméneur M, Erauso G, Postec A, Guentas-Dombrowski L, Payri C, Pelletier B. 2014. Fluid chemistry of the low temperature hyperalkaline hydrothermal system of Prony Bay (New Caledonia). Biogeosciences, 11: 5687–5706

Normand C, Williams-Jones A E, Martin R F, Vali H. 2002. Hydrothermal alteration of olivine in a flow-through autoclave: Nucleation and growth of serpentine phases. Am Mineral, 87: 1699–1709

Okamoto A, Ogasawara Y, Ogawa Y, Tsuchiya N. 2011. Progress of hydration reactions in olivine-H_2O and orthopyroxenite-H_2O systems at 250°C and vapor-saturated pressure. Chem Geol, 289: 245–255

Oufi O, Cannat M, Horen H. 2002. Magnetic properties of variably serpentinized abyssal peridotites. J Geophys Res: Solid Earth, 107: 2095, doi: 10.1029/2001JB000549

Oze C, Jones L C, Goldsmith J I, Rosenbauer R J. 2012. Differentiating biotic from abiotic methane genesis in hydrothermally active planetary surfaces. Proc Natl Acad Sci, 109: 9750–9754

Pan C C, Yu L P, Liu J Z, Fu J M. 2006. Chemical and carbon isotopic fractionations of gaseous hydrocarbons during abiogenic oxidation. Earth Planet Sci Lett, 246: 70–89

Schrenk M O, Kelley D S, Bolton S A, Baross J A. 2004. Low archaeal diversity linked to subseafloor geochemical processes at the Lost City Hydrothermal Field, Mid-Atlantic Ridge. Environ Microbiol, 6: 1086–1095

Schrenk M O, Brazelton W J, Lang S Q. 2013. Serpentinization, carbon, and deep life. Rev Mineral Geochem, 75: 575–606

Seyfried W E Jr, Pester N J, Ding K, Rough M. 2011. Vent fluid chemistry of the Rainbow hydrothermal system (36°N, MAR): Phase equilibria and *in situ* pH controls on subseafloor alteration processes. Geochim Cosmochim Acta, 75: 1574–1593

Sugisaki R, Mimura K. 1994. Mantle hydrocarbons: Abiotic or biotic?

Geochim Cosmochim Acta, 58: 2527–2542
Sun W D, Peng Z C, Zhi X C, Chen D G, Wang Z R, Zhou X H. 1998. Osmium isotope determination on mantle-derived peridotite xenoliths from Panshishan with N-TIMS. Chin Sci Bull, 43: 573–575
Tingle T N, Hochella M F Jr, Becker C H, Malhotra R. 1990. Organic compounds on crack surfaces in olivine from San Carlos, Arizona, and Hualalai Volcano, Hawaii. Geochim Cosmochim Acta, 54: 477–485
Toft P B, Arkani-Hamed J, Haggerty S E. 1990. The effects of serpentinization on density and magnetic susceptibility: A petrophysical model. Phys Earth Planet In, 65: 137–157
Ulmer G C. 1974. Alteration of chromite during serpentinization in the Pennsylvania-Maryland District. Am Mineral, 59: 1236–1241
Wang X B, Ouyang Z Y, Zhuo S G, Zhang M F, Zheng G D, Wang Y L. 2014. Serpentinization, abiogenic organic compounds, and deep life. Sci China Earth Sci, 57: 878–887
Wegner W W, Ernst W G. 1983. Experimentally determined hydration and dehydration reaction rates in the system MgO-SiO_2-H_2O. Am J Sci, 283-A: 151–180
Xiong Y Q, Geng A S, Wang Y P, Liu D H, Jia R F, Shen J G, Xiao X M. 2001. Kinetic simulating experiment on the secondary hydrocarbon generation of kerogen. Sci China Ser D-Earth Sci, 45: 13–20
Xu X S, Griffin W L, O'Reilly S Y, Pearson N J, Geng H Y, Zheng J P. 2008. Re-Os isotopes of sulfides in mantle xenoliths from eastern China: Progressive modification of lithospheric mantle. Lithos, 102: 43–64
Yang X Y. 2008. Geochemical study on Cenozoic mantle derived peridotitic xenoliths from Panshishan and Lianshan, Jiangsu Province. Dissertation for Master Degree. Guangzhou: Guangzhou Institute of Geochemistry, Chinese Academy of Sciences